



Preliminary results of a search for radio halos in starburst galaxies

C.A. Galante^{1,2}, J. Saponara², G.E. Romero^{1,2} & P. Benaglia²

¹ *Facultad de Ciencias Astronómicas y Geofísicas, UNLP, Argentina*

² *Instituto Argentino de Radioastronomía, CONICET-CICPBA-UNLP, Argentina*

Contact / camigalante04@gmail.com

Resumen / Las galaxias starburst atraviesan intensos episodios de formación estelar. En estas galaxias, el gas es eyectado al medio circundante en forma de vientos potentes producidos por el efecto combinado de numerosas explosiones de supernova. Cuando estos vientos interactúan con el medio intergaláctico pueden producir ondas de choque fuertes que son capaces de acelerar rayos cósmicos. La radiación de estos rayos cósmicos es producida por mecanismo sincrotrón y puede ser detectada en radio cuando las galaxias son vistas “edge-on” (es decir, cuando la inclinación de la normal a su plano orbital es $\sim 90^\circ$ con respecto a la visual). En este trabajo estudiamos una sub-muestra de galaxias edge-on del MeerKAT 1.28 GHz Atlas of Southern Sources in the IRAS Revised Bright Galaxy Sample. Para realizar un análisis de las galaxias individuales que nos permita encontrar emisión en radio por fuera del disco galáctico atribuible a la presencia del viento, se desarrolló y testeó un software que detallamos en este trabajo. Presentamos aquí los resultados obtenidos mediante este software para un sub-grupo de galaxias que han sido estudiadas en el pasado utilizando observaciones con baja resolución, comparando ambos casos.

Abstract / Starburst galaxies undergo intense episodes of star formation. In these galaxies, gas is ejected into the surroundings in the form of strong winds, produced by the combined effect of numerous supernova explosions. When these winds interact with the intergalactic medium, they give rise to strong shocks that are capable of accelerating cosmic rays. The radiation from these rays in radio wavelengths is generated by synchrotron mechanism and can be detected when the galaxies are seen “edge-on” (i.e., its inclination is $\sim 90^\circ$ with the line of sight). In this work, we investigate a sub-sample of edge-on galaxies in the MeerKAT 1.28 GHz Atlas of Southern Sources in the IRAS Revised Bright Galaxy Sample. To carry out an analysis of individual galaxies that allows us to find radio emission outside the galactic disk attributable to the presence of the wind, a software was developed and tested, which we detail in this work. We present here the results obtained using this software for a sub-group of galaxies that have been studied in the past using low-resolution observations, and we compare both results.

Keywords / galaxies: halos — galaxies: starburst — radio continuum: galaxies

1. Introduction

The extraplanar emission of starburst galaxies is produced by a strong wind powered by the intense star formation in the galactic disk. Cosmic rays accelerated in the wind or escaping from the galactic plane are responsible for non-thermal radio emission, which is produced by the synchrotron mechanism. Pioneering observations of edge-on galaxies (Hummel & van der Hulst, 1989; Hummel et al., 1991) clearly show that the radio continuum emission can extend far from the plane of the galaxy, up to distances of many kpc. The resulting “radio halo” is a tracer of the presence of the galactic wind well into the extragalactic space. In this work, we develop tools to detect and characterize radio halos in a sample of galaxies using a set of recent observations made with the MeerKAT* interferometer.

2. The sample

The IRAS Revised Bright Galaxy Sample (RBGS, Sanders et al., 2003) contains 629 galaxies observed by

IRAS with flux densities $S > 5.24$ Jy at $\lambda = 60 \mu\text{m}$ and galactic latitudes $b > 5^\circ$. The MeerKAT 1.28 GHz Atlas of Southern Sources in the IRAS RBGS (Condon et al., 2021) contains I-Stokes images of 298 RBGS southern galaxies with $7.5''$ angular resolution and rms of $20 \mu\text{Jy beam}^{-1}$. From this Atlas, we selected galaxies with inclinations $i > 80^\circ$. We identified them using INCLINET**, an online application for determining the inclinations of spiral galaxies from their optical images, which provides a reliable estimate of this parameter (Kourkchi et al., 2020). To ensure that the galaxies are resolved, we selected those whose angular sizes on the MeerKAT radio images are greater than 5 times the angular resolution in the direction perpendicular to the disk of the galaxy, calculated from the 3σ -contour. Applying these two selection criteria, we obtained a sample of 35 galaxies with distances between 3 and 53 Mpc.

3. Methodology

We prepared the MeerKAT images for analysis. We calculated an estimate of the rms by averaging all the

*<https://www.sarao.ac.za/science/meerkat/>

**<https://edd.ifa.hawaii.edu/inclinet/>

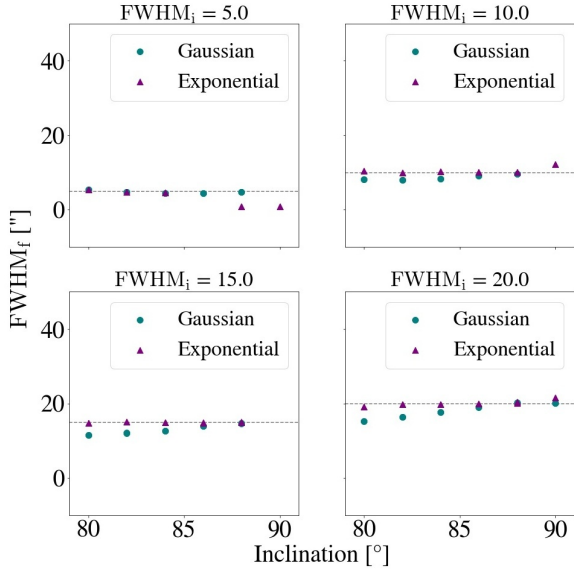


Figure 1: Halo FWHM obtained by our software for artificial galaxies built with different inclinations and halo FWHM, all with exponential-decaying disks (see text for details).

pixels whose intensity values were below three times the mean value of $20 \mu\text{Jy beam}^{-1}$ given by Condon et al. (2021), and defined the galaxy emission as the one above three times this quantity. We removed near non-related sources that may interfere with our analysis, and the central compact core in those galaxies where this latter emission is more than 25% of the total emission of the galaxy, using the NOD3 package (Müller et al., 2017).

The analysis was carried out by means of z -profiles, with z the direction normal to the galaxy plane. These profiles were obtained by averaging strips perpendicular to the galactic disk. The width of each profile is given by the effect of the beam of the telescope, the inclination of the galaxy, the intrinsic height of the galactic plane, and the possible presence of a radio halo. To model all these components, we first assumed that the galactic plane is an infinitesimally thin disk. When it is inclined and projected onto the sky, its profile along the z -direction can be described either by a Gaussian ($\omega_g(z) = \omega_0 \exp(-z^2/z_0^2)$) or an exponential function ($\omega_e(z) = \omega_0 \exp(-z/z_0)$), where z_0 is the scale height, which is independent of the sensitivity of the image. To model the effect introduced by the telescope resolution, each of these functions were convolved with a Gaussian-shaped beam. When one single function is not enough to fit the z -profile, a second exponential component was added to model the emission from the halo.

In order to verify that the method returns reliable results on the scale heights, we ran our software on a set of images of artificial galaxies with inclinations between 80 and 90 degrees with a two degrees step, which is the usual uncertainty for this parameter. These galaxies were computationally built pixel by pixel, as a two-dimensional array with 400 pixels per side. The intensity decay in the radial direction is described by an exponential function. Each of these values describes the maximum of a function -Gaussian or exponential- that

Table 1: Properties and results of the selected galaxies.

Name	D (Mpc)	i ($^\circ$)	$\langle z_h \rangle_D$ ($''$)	$\langle z_h \rangle_G$ ($''$)
NGC 1406	19	85	23	11.51
NGC 1421	21.2	82	0	12.51
NGC 3175	13.5	81	10.2	0
NGC 3717	21.4	85	0	0
NGC 5073	37.1	88	0	0
NGC 7090	7.7	88	31.2	19.3

describes the decay in z -direction. To create galaxies with halos, we added a second exponential component, with FWHM (Full Width at Half Maximum) between $5''$ and $20''$. Finally, we added Gaussian noise to the image. In this way, we obtained a set of 60 images with similar characteristics to the science images. In Fig. 1, each plot shows the fitted halo FWHM obtained with our software for artificial galaxies of different inclinations, all built with exponential disks and the same halo FWHM. In each plot, we show the results obtained fitting a Gaussian or an exponential disk. As can be seen, even when fitting Gaussian disks when the galaxies were built with exponential disks, the results are similar. This means that for a real galaxy, where we do not know a priori which is the real disk profile, we will never obtain a radio halo larger than its actual size.

4. First results

From our initial sample, we started analyzing a sub-set of galaxies that were studied before by Dahlem et al. (2001), hereafter DAL01. In their work, these authors analyzed 1.425 GHz Very Large Array (VLA) observations with $45''$ resolution and an rms of $\approx 90 \text{ Jy beam}^{-1}$ using a method similar to the one we approached in our work to obtain the halo scale heights. In Table 1 we present the galaxies, their distance D , their inclinations i , the halo scale heights obtained by DAL01 from VLA observations $\langle z_h \rangle_D$, and our results from the MeerKAT data $\langle z_h \rangle_G$. We could detect the presence of a radio halo for three of the six galaxies: NGC 1406, NGC 1421, and NGC 7090. We removed the central source according to the criteria defined in Sect. 3. Next, we highlight some aspects of the results that we obtained for each galaxy and compare them with the ones obtained by DAL01.

NGC 1406: both in DAL01 and this work, the z -profile could not be fitted with a single-component model, which indicates the presence of a radio halo. Although we obtained a smaller scale height, we arrived at the same relation between the scale height of the halo at both sides of the galactic plane, $z_{h,\text{left}}/z_{h,\text{right}}$. In DAL01, the authors mention that for this galaxy, observations with higher resolution are required to confirm the presence of the halo. In our work, using observations with a resolution six times higher, we confirm their preliminary result.

NGC 1421: in DAL01 the profile could be fitted by a single-component model. However, in our analysis, using observations with a higher angular resolution, we

found that it was necessary to add a second component to the fit. Evidence of a radio halo has already been detected for this galaxy in the past by Irwin et al. (1999); so we reinforce this result.

NGC 3175: for this galaxy, DAL01 found not very extended and low intensity deviations from a single-component function, but they mention that better resolution is required to confirm the presence of a halo. They perform the analysis, however, without removing the nuclear source –which according to the values obtained by Condon et al. (2021), contributes more than 25% to the integrated flux density– which can lead to interpreting the emission from the central source as the one from the disk, and a second component, corresponding to the disk, could mimic a radio halo. After removing it, we performed our analysis and found that the profile can be fitted with a single-component model, with no evidence of a radio halo. This difference can also be because the observations used by DAL01 had a poor angular resolution, so they may have included the emission of a near source as part of the galaxy. In fact, in the MeerKAT image of the galaxy, shown in Fig. 2, several particularly aligned blobs of emission are seen to the southeast of the galaxy. These features could be either part of the galaxy or non-related sources. In our analysis, we excluded this emission.

NGC 3717: our analysis of this galaxy agrees with the results found by DAL01, finding a single-component. These authors mention that the scale height found for the disk is unusually large compared to other galaxies, something that could indicate that indeed there is a halo but it cannot be separated from the disk emission. The MeerKAT image shows, however, that the emission of this galaxy follows the optical disk and is dominated by the nuclear source.

NGC 5073: it is the most distant galaxy studied by DAL01, who mention that the profile is almost non-resolved in z -direction. We found that a single-component fits the profile, with no evidence of a radio halo. From the MeerKAT image, it can be seen that the emission of this galaxy is resolved, following the optical disk, and it is dominated by the nuclear source.

NGC 7090: this galaxy shows asymmetric and prominent emission beyond the galactic disk. Both DAL01 and us agree about that a second component is necessary to describe its profile, and the presence of a radio halo is evident as can be seen in the z -profile shown in Fig. 3. As well as for NGC 1406, we found smaller scale heights for both sides of the radio halo, but the ratio $z_{h,left}/z_{h,right}$ was the same as the one found by these authors.

5. Conclusions and future work

We have selected and studied a sample of starburst galaxies observed by the MeerKAT radio interferometer, searching for the presence of extraplanar radio emission. To achieve our goal, we developed and tested a software that is capable of detecting the presence of this emission. We started analyzing a small sample of galaxies that were studied in the past with lower resolution observations. We found similar results to the previous

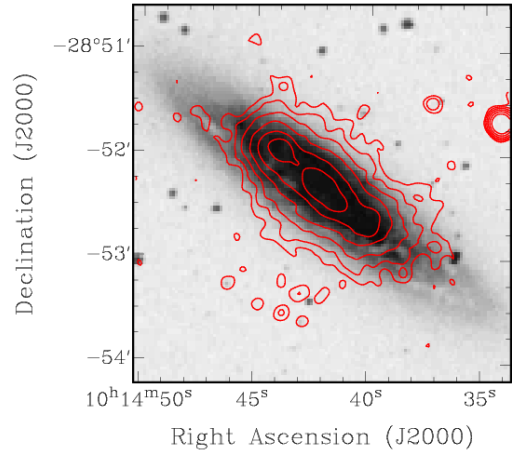


Figure 2: Radio continuum map overlaid on a DSS optical image of NGC 3175. Contours are at 3 (3σ), 6, 12, 24, 48, and $96 \times 20 \mu\text{Jy beam}^{-1}$.

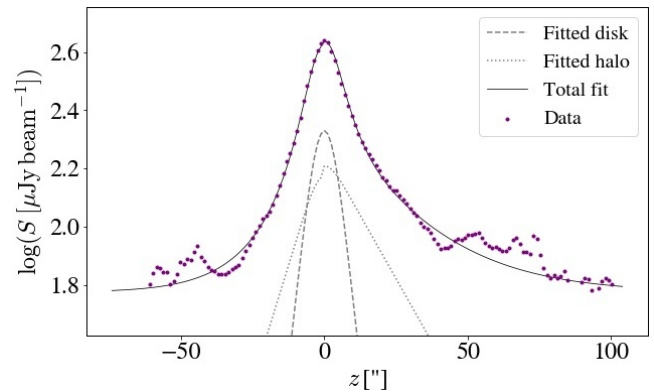


Figure 3: z -profile for NGC 7090. The fitted disk is shown in dashed line, while the halo component corresponds to the dotted line. The total model is plotted in bold line.

study for NGC 1406, NGC 3717, and NGC 7090. For NGC 3175 we could not detect the halo component that was previously claimed by DAL01. Our result, however, is stronger because of the better sensitivity and resolution of our data. For NGC 1421, finally, we detected the extraplanar emission that was missed in the low resolution images.

The next step in our research project is to complete the analysis of the remaining galaxies in our sample and perform statistical studies to search for possible correlations of the extraplanar emission with other properties of the galaxies.

References

- Condon J.J., et al., 2021, ApJS, 257, 35
- Dahlem M., et al., 2001, A&A, 374, 42
- Hummel E., Beck R., Dahlem M., 1991, A&A, 248, 23
- Hummel E., van der Hulst J.M., 1989, A&AS, 81, 51
- Irwin J.A., English J., Sorathia B., 1999, AJ, 117, 2102
- Kourkchi E., et al., 2020, ApJ, 902, 145
- Müller P., et al., 2017, A&A, 606, A41
- Sanders D.B., et al., 2003, AJ, 126, 1607